Uptake and retention of metals by cell walls of Bacillus subtilis.

T J Beveridge and R G Murray
J. Bacteriol. **1976, 127(3):1502.**

JOURNAL OF BACTERIOLOGY, Sept. 1976, p. 1502-1518
Vol. 127, No. 3

Printed in U.S.A.

Uptake and Retention of Metals by cell Walls of *Bacillus subtilis*

T. J. BEVERIDGE* AND R. G. E. MURRAY

Department of Bacteriology and Immunology, University of Western Ontario, London, Ontario, Canada

Received for publication 30 April 1976

Isolated walls of *Bacillus subtilis* Marburg, prepared in a manner which avoided metal contamination other than by the growth medium, were incubated in dilute metal solutions, separated by membrane filtration (0.22 μm), and monitored by atomic absorption to give uptake data for 18 metals. Substantial amounts of Mg^{2+}, Fe^{3+}, Cu^{2+}, Na^{+}, and K^{+} (amounts which were often visible as electron scattering in thin sections), intermediate amounts of Mn^{2+}, Zn^{2+}, Ca^{2+}, Au^{3+}, and Ni^{2+} (the higher atomic-numbered elements also visible as electron scattering), and small amounts of Hg^{2+}, Sr^{2+}, Pb^{2+}, and Ag^{+} were taken into the wall. Some (Li^{+}, Ba^{2+}, Co^{2+}, and Al^{3+}) were not absorbed. Most metals which had atomic numbers greater than 11 and which could be detected by electron microscopy appeared to diffusely stain thin sections of the wall. Magnesium, on the other hand, partitioned into the central region, and these sections of walls resisted ruthenium red staining, which was not true for the other metals. Areas of the walls also acted as nucleation sites for the growth of microscopic elemental gold crystals when incubated in solutions of auric chloride. Retention or displacement of the metals was estimated by a "chromatographic" method using the walls cross-linked by the carbodiimide reaction to adipic hydrazide agarose beads (which did not take up metal but reduced the metal binding capacity of the walls by ca. 1%) packed in a column. When a series of 12 metal solutions was passed through the column, it became evident that Mg^{2+}, Ca^{2+}, Fe^{3+}, and Ni^{2+} were strongly bound to the walls and could be detected by both atomic absorption and by their electron-scattering power in thin sections, qhereas the other metals were fisplaced or replaced. Partial lysozyme digestion of the walls (causing a 28% loss of a [^{3}H]diaminopimelic acid label) greatly fiminished the Mg^{2+} retention but not that of Ca^{2+}, Fe^{3+}, or Ni^{2+}, indicating that there are select sites for various cations.

It is well known that some metals (e.g., Mo, Fe, Mg, Ca, K, etc.) are concentrated from the environment by microorganisms or are actively sequestered by organic chelating agents, such as the exochelins, to satisfy the specific requirements of metal-enzymes and/or structural components (5, 6, 8, 22, 28, 30, 36, 45). Some, such as Fe or Mn, are precipitated as insoluble oxides or hydroxides in extracellular sheaths (37, 38) and lead to metal-rich deposits. Certainly Mg^{2+} is required for the assembly and stability of the plasma membrane of bacteria (15) and for the outer membrane of the gram-negative wall (22, 27), and Ca^{2+} or Sr^{2+} is required for the integrity and attachment of superficial cell wall layers (5, 6, 8). The ash of some wall constituents such as the murein of *Klebsiella pneumoniae* (16) and a marine pseudomonad (47) contain cationic species, particularly Ca^{2+} and Mg^{2+}. All these and many other such observations (21, 26, 40, 41) indicate that there may be rather specific mechanisms and sites in the bacterial envelope for the trapping of metals; yet remarkably little in the way of physicochemical data seems to be available, nor have model systems been developed to explore the mechanisms and specificities of interaction.

The most durable anionic organic constituents of bacteria are provided by the structural polymers of the cell wall which are, in general, complex polyanions and would seem to offer likely sites for the trapping of metal cations. We have set out to develop a simple set of methods for studying this trapping phenomenon using isolated cell walls of *Bacillus subtilis* as representative of the kinds of durable organic polyanions we need for a model.

MATERIALS AND METHODS

Precautions taken to prevent metal contamination during experiments. Metal contamination from glassware is a hazard for accurate inorganic analy-

ses and for this reason only plasticware, which had been previously leached of contaminating metals by overnight concentrated HNO_3 (reagent grade, McArthur Chemical Co., Montreal, Canada) treatment, was used throughout the experiments. With the exception of the growth flask (which was glass), only polypropylene or TPX-nalgene (Nalge Sybron Corp., Rochester, N.Y.) containers were used. The water, which was double distilled and deionized, and all reagents were checked by flame atomic absorption analysis for metal contamination before each experiment.

Preparation of cell wall fragments. Thirty milliliters of an exponentially growing culture of *Bacillus subtilis* Marburg cells (University of Western Ontario collection no. 1032) was inoculated into a 6-liter flask containing 3 liters of NSMP medium which contained, per liter: 8 g of nutrient broth (Difco Laboratories, Detroit, Mich.), 20 mg of DL-methionine (Fisher Scientific Co., Pittsburgh, Pa.), 25 mg of L-tryptophan (Fisher), and 10 g of D-glucose (Difco) as organic supplements; $CaCl_2$ (Sigma), $MgCl_2$ (Sigma), $MnCl_2$ (Fisher), and $FeCl_3$ (Fisher) as a salt mixture; and mono- and dibasic potassium phosphate as a buffering agent (18). After incubation at 22°C for 12 h on a rotary shaker, this medium produced an exponential, nonsporulating culture with a Klett reading of 214 (Klett-Summerson photoelectric colorimeter, Klett Manufacturing Co., Inc., New York, N.Y.). The cells were harvested and washed twice in deionized distilled water (DDW), resuspended in 0.05 M *N*-2-hydroxyethylpiperazine-*N'*-2-ethanesulfonic acid (HEPES) buffer (A grade; Calbiochem, Los Angeles, Calif.) adjusted to pH 7.2 with 1 N NH_4OH (reagent grade, the British Drug Houses [Canada] Ltd., Toronto, Canada) and broken by using a French pressure cell (American Instrument Co., Inc., Silver Spring, Md.) operating at 20,000 lb/in^2.

The envelopes were separated centrifugally (10,000 × *g*, 30 min) after removal of the unbroken cells (3,000 × *g*, 30 min), resuspended in 50 ml of HEPES buffer, and immediately heated to 100°C for 10 min to denature autolysins. The subsequent washings (two times), treatment with 50 μg of deoxyribonuclease per ml at pH 4.5 with 1 mM $MgCl_2$ for 3 h at 25°C, further washing (two times) and treatment with 100 μg of ribonuclease per ml at pH 7.2 for 3 h at 37°C, and washing until the optical absorbance at 260 nm approached zero were all performed with 50-ml volumes of HEPES buffer (all chemical and enzyme additives from Sigma). The fragments were next suspended in HEPES buffer to give a Klett reading of ca. 150, and a 1-ml portion was layered on top of a 10-50-60-70% discontinuous gradient (2 ml of each concentration) using sucrose of density gradient grade (Schwarz/Mann, Div. of Becton, Dickinson & Co., Orangeburg, N.Y.) mixed in HEPES. This gradient was then centrifuged for 30 min at 12,000 × *g* using an HP-4SB Sorvall centrifuge head (Ivan Sorvall, Inc., Norwalk, Conn.). The band at the 50 to 60% interface was collected and dialyzed overnight at 4°C in 2 liters of HEPES, followed by an 8-h dialysis in 2 liters of DDW at 4°C, after which the dialysate was lyophilized. Repetition of this technique provided almost 50 mg (dry weight) of wall material from the 3 liters of culture. The purity of the wall fragments was ascertained by electron microscopy (negative stains and thin sections) and testing for reduced nicotinamide adenine dinucleotide oxidase as a marker for plasma membrane enzymes (42).

Preparation of [^{3}H]DAP-labeled wall fragments. Cells were cultured through 60 generations in four changes of 100 ml of NSMP medium containing 2 μg of DL-methionine per ml, 2.5 μg of L-tryptophan per ml, 10 mg of D-glucose per ml, 100 μg of L-lysine (Sigma Chemical Co., Detroit, Mich.), 100 μg of DL-α,ε-diaminopimelic acid (DAP) (Sigma) per ml. Thirty milliliters of an exponentially growing culture was inoculated into 3 liters of NSMP medium supplemented with 16.5 μg of L-lysine per ml and 0.66 μCi of [^{3}H]DAP per ml {(DL + *meso*)-2,6-diamino[G-^{3}H]pimelic acid dihydrochloride; specific activity, 300 mCi/mmol; Amersham/Searle Corp., Des Plains, Ill.} and grown for 12 h at 22°C on a rotary shaker. Wall fragments were prepared as described.

Incorporation of [^{3}H]DAP into the wall fragments was estimated using hyamine (1 M hyamine in methanol; Packard Instrument Co., Inc., Downers Grove, Ill.) digested walls by liquid scintillation counting in a Beckmann liquid scintillation counter model LS-250 (Beckman Instruments, Inc., Fullerton, Calif.). A scintillation fluid composed of 4 g of PPO (2,5-diphenyloxazole) plus 0.1 g of dimethyl POPOP 1,4-bis-[2-(4-methyl-5-phenyloxazolyl)]-benzene (both scintillation grade; Packard) per liter of toluene (scintillation grade; Fisher Scientific Co.) was used as the scintillation cocktail.

Reduced nicotinamide adenine dinucleotide oxidase detection. This assay was done according to Osborn et al. (42) using a Gilford 2400 recording spectrophotometer (Gilford Instruments Laboratories, Inc., Oberlin, Ohio) to test 10- to 100-μg (dry weight) quantities of either: (i) purified wall fragments, (ii) crude wall fragments (a preparation of mechanically disrupted cells which has had the unbroken cells removed by centrifugation and which thin sections indicated possessed plasma membrane), or (iii) reduced nicotinamide adenine dinucleotide oxidase of known specific activity (Diaphorase, pig heart; specific activity, 3.1 μmol/mg of protein per min; Sigma). In all cases the reaction could be completely inhibited by 10 mM cyanide.

Uptake analyses using either cold or [^{3}H]DAP-labeled wall fragments. The following salts were used for metal uptake studies: LiCl, NaCl, KCl, $SrCl_2 \cdot 6H_2O$, $BaCl_2 \cdot 2H_2O$, $MnCl_2 \cdot 4H_2O$, $FeCl_3 \cdot 6H_2O$, $CoCl_2$, $Ni(NO_3)_2 \cdot 6H_2O$, $CuCl_2 \cdot 2H_2O$, $AgNO_3$, $ZnCl_2$, $Al_2(SO_4)_3 \cdot 18H_2O$, $Pb(NO_3)_2$, $HgCl_2$ (all reagent grade; Fisher Scientific Co.); $CaCl_2$, $MgCl_2 \cdot 6H_2O$ (Sigma), and $AuCl_3 \cdot 2H_2O$ (K & K Laboratories, Inc., Jamaica, N.Y.).

One milliliter of a 10 mM solution of a metal salt was combined with 1 ml of DDW containing 0.5 mg (dry weight) of the wall fragments per ml in a 10-ml disposable plastic syringe (Plastipak, Becton-Dickinson & Co., Mississauga, Ontario, Canada) and reacted for 10 min with continuous agitation with the plunger pulled back to the 5-ml position. Experi-

ments with $AgNO_3$ and $AuCl_3 \cdot 2H_2O$ were performed in the dark. The suspension was then separated using a 0.22-μm membrane filter (Millipore Corp., Bedford, Mass.) contained in a 25-mm polypropylene Swinnex filter holder (Millipore), and the filtrate was collected in a 100-ml TPX Nalgene beaker. Two volumes of 10 ml of DDW was taken into the syringe (without filter attachment) and agitated for 5 min, and each of these was forced through the original filter. Thirty milliliters of DDW was next forced through the filter to wash any unbound metal salt into the filtrate (all filtrates were combined). The combined filtrate was heat dried, and the residue was treated with 20 ml of concentrated HNO_3 which was heated to dryness. Twenty milliliters of HNO_3 was used in the same manner to hydrolyze the filter plus wall fragments. Controls, in which 1 ml of DDW was substituted for the wall suspension, were treated in exactly the same manner. All hydrolysates were dissolved in 0.15 N HNO_3 containing 1,000 μg of CsCl per ml (Fisher Scientific Co.), and these solutions were used for atomic absorption analyses. Metal uptake was estimated by determining the amount of metal on each Millipore filter and validated by determining the amount in the filtrate. Both filtrate and filter analyses had to equal ($\pm$1%) the total available metal for the experiment to be termed valid, and each experiment was repeated at least twice. Those metals with high uptake values were repeated several times.

Atomic absorption analyses were performed with a Perkin-Elmer model 403 atomic absorption unit (Perkin-Elmer Canada Ltd., Downsview, Ontario, Canada) by either flame or graphite furnace (HGA graphite furnace attachment; Perkin-Elmer Canada Ltd.) absorption using appropriate hollow cathode lamps for the metals. All metal salts, HNO_3, and plasticware were analyzed for background contamination, as were the cell wall preparations and the DDW.

Electron microscopy of metal uptake reaction mixtures. The walls were treated as described in the uptake experiments, except that after the washing procedure they were scraped from the Millipore filter and fixed in 4% glutaraldehyde (EM grade, Polysciences Inc., Warrington, Pa.) in DDW for 1 h at 22°C (atomic absorption analysis indicated that the glutaraldehyde was free from metal contamination) and washed by centrifugation in 3× 10 ml of DDW. The walls were next enrobed in Noble agar (Difco), dehydrated through an acetone series, embedded in Vestopal W (Martin Jaeger, Vesenaz, Geneva, Switzerland), and sectioned on a Reichert model OMU2 ultramicrotome, and silver sections were collected on carbon-Formvar-coated 200-mesh grids. No stains were applied to the sections for the initial detection of metal by electron microscopy. In several instances ruthenium red (500 μg per ml of DDW) (Polysciences Inc.) or uranyl acetate followed by lead citrate (48) were used to stain the sections on the grids to ascertain the "stainability" of the walls after their metal incubations.

X-ray analysis for elemental gold in wall fragments. The wall fragments were incubated in a 5 mM solution of $AuCl_3 \cdot 2H_2O$ in the dark and embedded as if for sectioning. A 1-mm^3 block of Vestopal W-embedded wall fragments were used as the specimen, mounted on a glass fiber, suspended in the center of a Gandolfi Powder Camera (diameter, 57.3 mm), and analyzed using filtered Fe K alpha radiation. The identification of metallic gold was obtained by comparison to the Joint Committee on Powder Diffraction Standards file (1974) for this element.

Preparation of F-Con A for electron microscopy. The conjugation of ferritin (General Biochemicals Div. [Mongul Corp.], Chagrin Falls, Ohio) to concanavalin A (F-Con A) (Nutritional Biochemicals Corp., Cleveland, Ohio) was accomplished by the method of Nicolson and Singer (39), and the active fraction was purified as described by Agrawal and Goldstein (1).

Electron microscopy using F-Con A. The reactivity of the conjugate was assessed by mixing a 0.1-ml suspension of wall fragments (0.5 mg [dry weight]/ml) with 0.1 ml of the F-Con A (1 mg of protein per ml), incubating at 22°C for 60 min with continuous agitation, and washing the wall fragments five times with 5 ml of 0.5 M NaCl-0.05 M sodium phosphate buffer, pH 6.8. These walls were layered on a carbon-Formvar-coated grid, scanned with an electron microscope, and compared to a control mixture which contained either 0.1 M D-glucose (Fisher Scientific Co.) or 0.1 M α-methyl-D-mannoside (Sigma) as specific blocking agent.

The wall fragments, after incubation with metal salts, were treated as previously described for the electron microscopy of metal uptake reaction mixtures, except that after the metal washing procedure the walls were resuspended in 0.1 ml of DDW and mixed with 0.1 ml of F-Con A in 1 mM phosphate-buffered saline (phosphate-buffered saline concentration was lowered by dialysis) and the reaction mixture was continuously agitated for 60 min at 22°C. The qalls were then pelleted by centrifugation, washed five times with 10-ml volumes of DDW, fixed for 60 min at 22°C with 4% glutaraldehyde (Polysciences Inc.), and processed for sectioning as previously described.

Binding of wall fragments (cold or [^{3}H]DAP labeled) to adipic hydrazide agarose. Adipic hydrazide agarose (AHA) (Miles Laboratories, Inc., Elkhart, Ind.) was dialyzed overnight at 4°C in 6 liters of DDW to remove the toluene preservative. Ten milligrams (dry weight) of wall fragments was added to 20 ml of AHA, the slurry was adjusted to pH 5.0 with 1 N HCl, and enough 1-ethyl-3-(3-dimethylaminopropyl)carbodiimide hydrochloride)edc, Storey Chemical Corp., Muskegon, Mich.) was added to make the mixture 0.1 M. This reaction mixture required slow stirring and was monitored for pH fluctuations (adjustments made with 0.1 N HCl) until the pH stabilized (ca. 1 h after initiation of reaction), and the reaction continued for 24 h at 22°C after which the slurry was allowed to settle by gravity, the suspending fluid was aspirated, and the beads were washed with 50 ml of DDW 5 times to remove unabsorbed wall fragments.

Metal retention studies. Twenty milliliters of the AHA slurry with bound wall fragments (AHA-WF)

was poured into an acrylic chromatographic column (1 by 25 cm^3) equipped with a Teflon stopcock plug (Nalge Sybron Corp.) and previously leached with HNO_3, and was retained by a 0.45-μm membrane filter (Millipore) supported on a 1-cm Swinnex filter grid (taken from a 13-mm polypropylene Swinnex filter holder; Millipore) immediately above the outlet (column no. 1). After the slurry had settled (settled volume, 10 ml) the column was washed with 200 ml of DDW. These preparatory steps and the following experiment were performed at 4°C, and all plasticware had been previously leached with concentrated HNO_3.

A series of metal salts was added in the following manner. A 1-ml portion of a 5 mM solution was layered on top of the column, allowed to run into the AHA-WF matrix, and immediately chased with 50 ml of DDW to wash unabsorbed metals from the column, and the effluent was collected in a 250-ml TPX Nalgene beaker. Once the DDW had reached the column surface, the effluent flow was stopped, another collecting beaker was placed under the column nozzle, a different 5 mM metal solution (1 ml) was layered on top, and the flow once again was started. This process was repeated until 10 metal solutions had been run through the column. The order of the application to the column was as follows: $NaCl \rightarrow KCl \rightarrow MgCl_2 \cdot 6H_2O \rightarrow CaCl_2 \rightarrow BaCl_2 \cdot 2H_2O \rightarrow FeCl_3 \cdot 6H_2O \rightarrow CuCl_2 \cdot 2H_2O \rightarrow CoCl_2 \rightarrow MnCl_2 \cdot 4H_2O \rightarrow Ni(NO_3)_2$.

Two control columns were used for this experiment, and the same experimental procedures and sequence of metals were applied to them; column no. 2 contained AHA-WF ([^{3}H]DAP labeled) and column no. 3 contained AHA alone (i.e., without attached wall fragments). In column no. 2 the effluent in each beaker was heated to dryness, the residue was digested with hyamine, and [^{3}H]DAP was estimated by liquid scintillation to obtain an index of any cell wall degradation during the experiment. In column no. 3, the effluents and column matrix provided atomic absorption background readings for AHA and the acrylic of the column. The matrix was processed in parallel to that of column no. 1 as follows. After the experiment the slurry from each column was hydrolyzed with 20 ml of concentrated HNO_3 and heated to dryness. The collecting beakers from the columns, which each contained 51 ml of effluent, were heated to dryness, and the residue was hydrolyzed in the same manner as described for the column slurries. The hydrolysates were redissolved in 0.15 N HNO_3 containing 1,000 μg of CsCl per ml, and each was analyzed by atomic absorption for all 10 metals. Metal retention was estimated by determining the amount of each metal in the slurry and applying this value to the amounts in the effluents. For the experiment to be valid the amount of each metal in the slurry combined with the amount in the effluents must equal (±1%) the total available.

Metal retention of wall fragments partially digested by lysozyme. Three columns were used in this experiment; all columns were packed as described previously, two (no. 4 and no. 5) with AHA-WF and one (no. 6) with AHA-WF ([^{3}H]DAP labeled). After being packed and washed, all three columns were brought to 22°C, and a 10-ml solution containing 25 μg of lysozyme (Sigma) per ml was run into columns no. 4 and no. 6. After a 2-h incubation period all columns were washed with 100 ml of cold DDW, the effluent of column no. 6 was collected (and processed for an estimation of [^{3}H]DAP leakage as previously described), and all columns were brought back to 4°C. The same series of metal salts and procedures as previously described for metal retention studies was applied to each column.

Column no. 4 was used to obtain metal retention values for fragments partially digested by lysozyme, column no. 5 was an undigested control column, and column no. 6 was used to establish an estimate of cell wall disruption by the lysozyme as well as from each metal as it was put through the column.

Electron microscopy of metal retention experiments. In several instances 0.05-ml portions were taken from the columns used in the metal retention studies of whole wall fragments and partially digested fragments, and these were fixed for 60 min at 22°C with 4% glutaraldehyde in DDW. These were next washed five times with 5 ml of DDW by centrifugation at 750 × *g* (higher centrifugal force collapsed the AHA beads) and processed as previously described for thin sections.

RESULTS

Metal uptake experiments. There were three bands after discontinuous sucrose gradient centrifugation of the crude wall preparation: band no. 1 at the sample-10% sucrose interface; no. 2 at the 10 to 50% interface; and no. 3 at the 50 to 60% interface; and a pellet at the end of the tube. Negative stains of interface no. 1 revealed small membrane vesicles and particulate debris (ribosomes?); of no. 2, small cell wall fragments which were often associated with membrane material; of no. 3, large wall fragments consisting of polar ends and cross walls; and of the pellet, unbroken cells. Thin sections of interface no. 3 demonstrated large wall fragments which were free from plasma membrane and cytoplasmic contamination (Fig. 1 and 2A), and tests on these fragments for reduced nicotinamide adenine dinucleotide oxidase activity (a plasma membrane enzyme of *Bacillus subtilis* [31]) suggested that this wall fraction had undetectable activity when compared to a crude wall preparation which contained membrane (e.g., this crude preparation had 0.33×10^{-3} μM activity/mg [dry weight] per min when compared to diaphorase).

Atomic absorption analyses of these wall fragments suggested that they were in the magnesium form, presumably due to the Mg^{2+} in the growth medium, and contained, respectively, 0.12 μmol of Mg^{2+} and 0.02 μmol of K^+ per mg (dry weight) of cell wall material. The other supplementary metals (Ca^{2+} and Fe^{3+}) were undetectable in the walls by this technique.

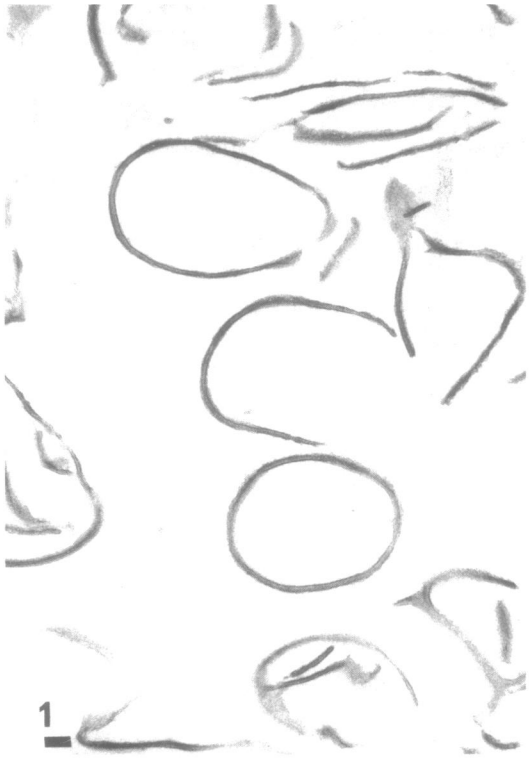

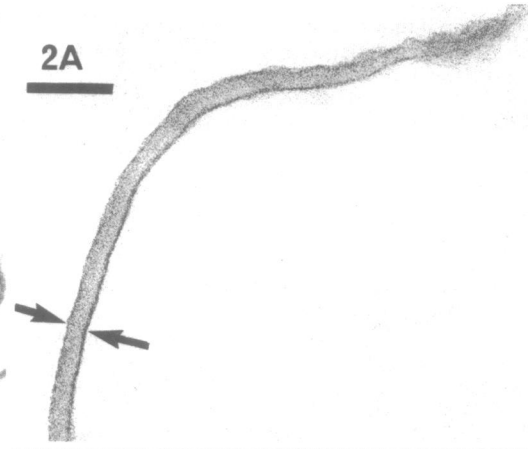

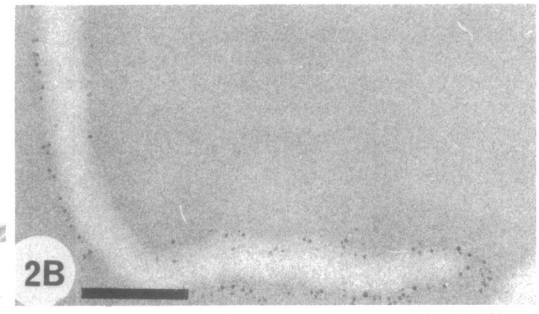

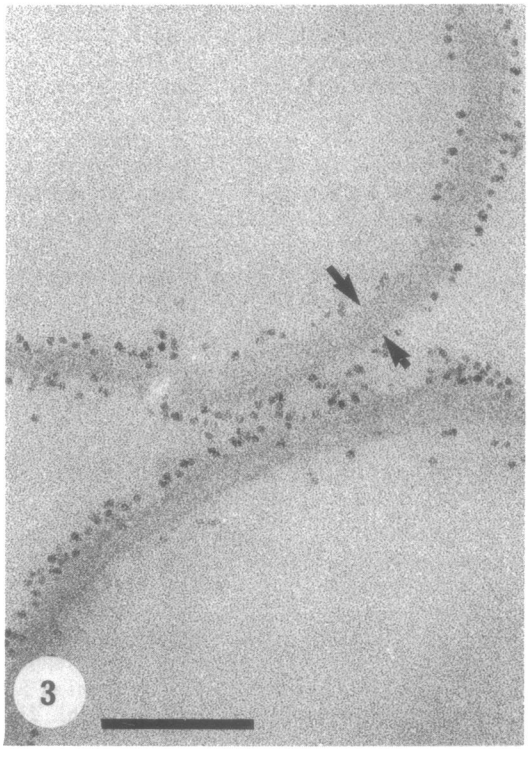

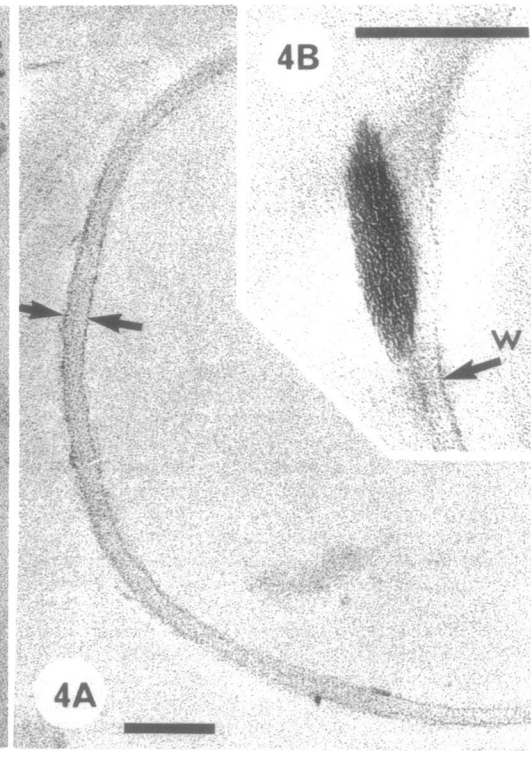

Wall fragments which were incubated in the various metal solutions for 10 min at 22°C gave the metal uptake values found in Table 1 and, in the cases of Mg^{2+}, Cu^{2+}, Mn^{2+}, Zn^{2+}, Fe^{3+}, or Au^{3+} incubations, the walls became visible by electron microscopy (compare Fig. 2B with 3, 4A, 7 and 13) presumably due to the electron-scattering power of the absorbed metal. In most cases (with the exception of Mg^{2+} and Au^{3+}) the walls were diffusely stained by the metals (Fig. 3), although in the case of Fe^{3+} both inner and outer surfaces appeared slightly more dense (Fig. 4A), but this could be due to a penetration problem for the metal. Walls stained with these metals when measured had a width comparable to those which had been stained with uranyl acetate and lead citrate (compare Fig. 2A, 3, and 4A; arrows indicate 25-nm widths in each wall fragment). The walls which were incubated with Fe^{3+} occasionally revealed dense crystaloids on the wall surfaces which had a definite lattice network (Fig. 4B is representative).

On the other hand, although Mg^{2+} had a large uptake value (Table 1) the walls showed extremely slight contrast (presumably due to the metal's low atomic number), and this metal appeared to delineate the central region of the cell wall (Fig. 7). Measurements of cross-sectioned walls indicated that this region extended 16 nm in width, diffusely scattered electrons, and lay 5 to 9 nm from both inner and outer wall surfaces (i.e., the less dense spaces which enclose this urea). Thin sections stained by Reynolds' method (48) indicated that walls not suspended in the Mg^{2+} solution had a minimum width of 25 nm, usually at the polar cap, and a maximum of 35 nm, usually along the cross wall)fig. 1 and 2A are representative). The measurements of the apparent thickness of Mg^{2+}-incubated walls fell within these limits but, since we had no definite surface label for these sections of walls, we could not rule out

TABLE 1. *Uptake values of B. subtilis wall fragments for metals as determined by atomic absorption analysis after a 10-min incubation at 22°C in a 5 mM metal solution*

Metal	Uptake	
	μg/mg (dry wt) of wall fragments	μmol/mg (dry wt) of wall fragments
Li^{+}	0	0
Na^{+}	62.0	2.697
K^{+}	76.0	1.944
Mg^{2+}	200.0	8.226
Ca^{2+}	16.0	0.399
Sr^{2+}	2.4	0.027
Ba^{2+}	0	0
Mn^{2+}	44.0	0.801
Fe^{3+}	200.0	3.581
Co^{2+}	0	0
Ni^{2+}	6.3	0.107
Pb^{2+}	4.1	0.020
Cu^{2+}	190.0	2.990
Ag^{+}	3.8	0.035
Au^{3+}	71.4	0.363
Zn^{2+}	45.8	0.701
Hg^{2+}	8.04	0.040
Al^{3+}	0	0

artifacts (e.g., the possibility of expansion induced by the electron beam and/or the contraction of the wall-Vestopal W interface). The possibilities were tested in two ways: (i) using the electron scattering, nonpenetrating, and wall-specific label provided by F-Con A; and (ii) using no stain except for Mg^{2+} until after sectioning and then treating the section with either uranyl acetate-lead citrate or ruthenium red. After these stains there should be a doubling effect between the Mg^{2+} and the applied stain, thereby accentuating the location of the magnesium.

Experiments involving incubation of walls with F-Con A (Fig. 5) or F-Con A blocked with either D-glucose or α-methyl-D-mannoside in the reaction mixture (Fig. 6) demonstrated that the F-Con A attached to the wall and that the specificity was presumably directed at the α-D-

FIG. 1. *Low magnification view of a thin section containing some of the wall fragment fraction used for the metal interaction studies. This and Fig. 2 are stained with uranyl acetate-lead citrate. The marker bar in this and the following micrographs represents 100 nm unless otherwise stated.*

FIG. 2. *(A) Higher magnification of a sample similar to Fig. 1 which shows a polar (end wall) fragment. Width of wall between the arrows is 25 nm. (B) Similar to Fig. 2A but unstained, except by particles of F-Con A that outline the wall surfaces. Note that the wall substance is less dense than the Vestopal W embedding substance.*

FIG. 3. *Thin section of wall fragments after incubation in 5 mM $ZnCl_2$ for 10 min at 22°C which show a diffuse opacity in the wall substance. The wall surfaces have been labeled with F-Con A to emphasize the location of the walls and no stain other than Zn^{2+} has been used. The distance between arrows is 25 nm.*

FIG. 4. *(A) Thin section of a wall fragment after 5 mM Fe $Cl_3 \cdot 6H_2O$ incubation for 10 min at 22°C. No stain other than Fe^{3+} has been used. The wall surfaces show distinct density, and the rest of the wall substance is diffusely stained by the iron. The distance between the arrows is 25 nm. (B) High magnification of a wall-associated "crystaloid" from the same preparation as Fig. 4A showing a lattice network. No stain has been used.*

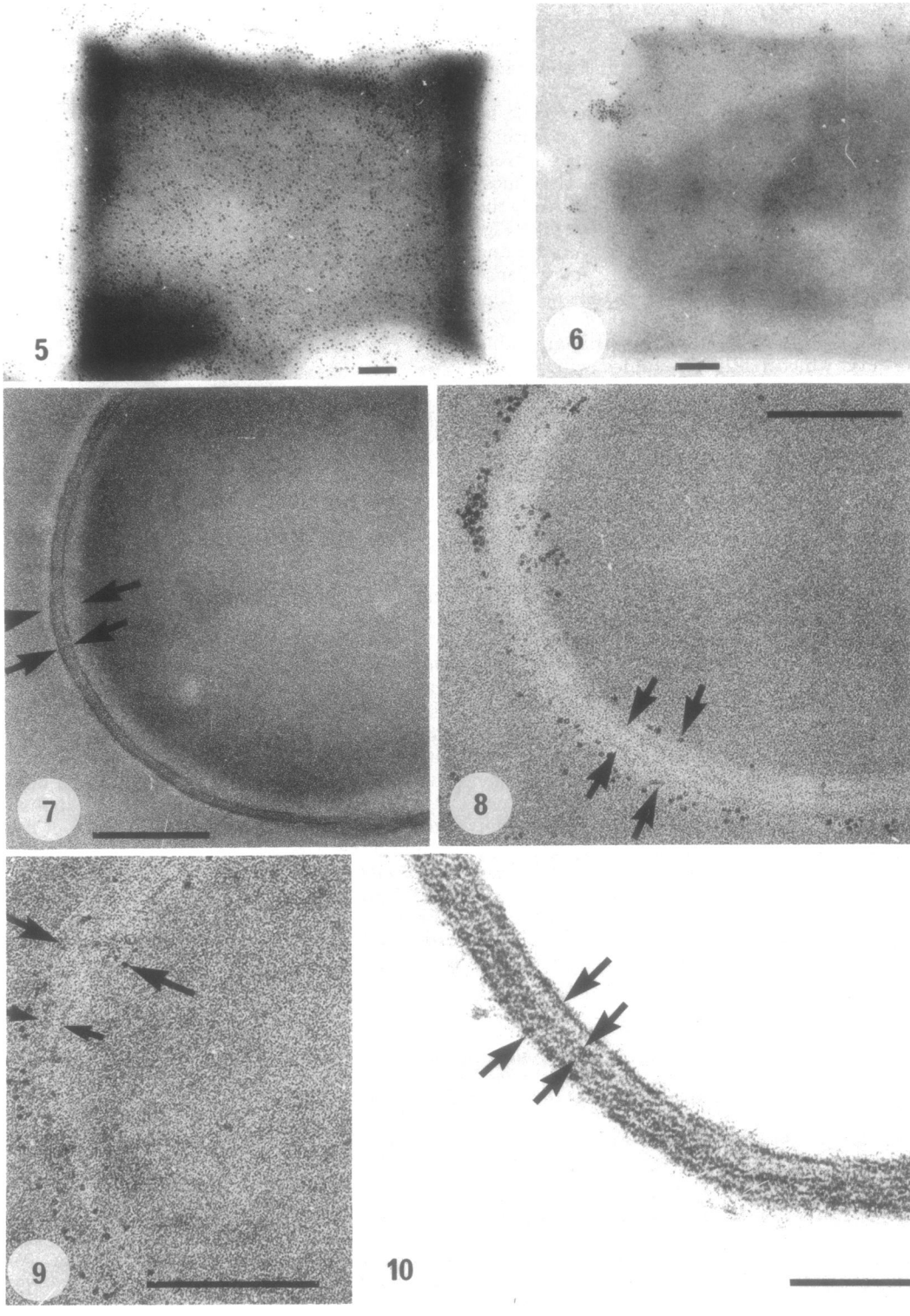

glucose residues of the wall-bound teichoic acid (7, 11). Sections of walls treated with F-Con A alone demonstrated attachment on both inner and outer wall surfaces, with a minimum separation of 30 nm for polar cap wall and 40 nm for cross wall (Fig. 7). Wall fragments which were incubated in Mg^{2+}, washed, and then treated with F-Con A showed a definite displacement of the ferritin particles from the double track of absorbed Mg^{2+} (Fig. 8).

Two independent stains were applied to sections of untreated and Mg^{2+}-treated walls. Ruthenium red is specific for acid mucopolysaccharides (35) and, in this case, would be expected to attach to teichoic acid (19). Reynolds' uranyl acetate-lead citrate (48) is a nonspecific stain for the anionic groups of the section (23). When walls incubated in Mg^{2+} were sectioned and stained with ruthenium red the staining reaction was questionable (Fig. 9). Although some density was contributed by the stain, it was not of the same order as seen in walls not treated with Mg^{2+} or in walls which were incubated in other metal solutions. On the other hand, Reynolds' stain imparted high contrast to the wall (Fig. 10), and the doubling effect of the stain on the bound Mg^{2+} was very apparent (see small spacing aspect, Fig. 10). With both stains the wall exhibited total widths of 25 to 35 nm, and this confirmed the localization of the Mg^{2+} into a central region of the cell wall.

Wall fragments that had been treated with $AuCl_3 \cdot 2H_2O$ revealed small (5 to 25 nm), extremely dense granules within the wall substance after a 5-min incubation (Fig. 11), and within 10 to 15 min these granules had grown and exhibited definite geometrical shapes almost obliterating the image of the cell wall (Fig. 13). Examination of the crystal form and X-ray diffraction of the wall fragments (Fig. 12) revealed that these dense granules were elemental gold.

Of the wall fragment preparations tested, the electron-scattering ability was as follows: $Au^{3+} >> Fe^{3+} > Zn^{2+} > Mg^{2+} > Na^+ = K^+ = Cu^{2+} = Mn^{2+} > Ca^{2+} = Ni^{2+} > Hg^{2+} = Ag^{2+} = Pb^{2+} = Co^{2+} = Ba^{2+} = Sr^{2+} = Al^{3+} = Li^+ = O$. Once sectioned, all of these preparations were amenable to uranyl acetate-lead citrate staining and, with the exception of the Mg^{2+}-reacted walls, to ruthenium red staining.

Walls were incubated in varying concentrations of either Mg^{2+} or Fe^{3+} for 42 h at 4°C (to discourage bacterial contamination), and uptakes were calculated (Table 2). Exposure to 5 mM concentrations of the two metals for this extended period provided lower uptake values than had been found after a 10-min incubation at 22°C. There appeared to be a relatively small increase in the Mg^{2+} uptake for a 100-fold increase in the initial metal concentration, i.e., about 30% on a molar base. Thin sections of these walls demonstrated the same Mg^{2+} partitioning as previously described, although this was harder to demonstrate with the 0.5 mM incubation (presumably this Mg^{2+} uptake concentration was approaching the limits of electron-scattering power). Wall fragments that were incubated in the Fe^{3+} solutions demonstrated a drastic decrease in metal uptake, but this uptake appeared to be concentration dependent (Table 2). Thin sections of these walls revealed numerous dense crystaloids (similar to that seen in Fig. 4B) attached to wall fragments as well as scattered throughout the embedding medium. The walls had less electron-scattering power than that observed in Fig. 4, and this, no doubt, was due to decreased uptake.

When [^{3}H]DAP-labeled fragments were used in the 10 min at 22°C or the 42 h at 4°C metal uptake experiments and the filtrate was monitored for radioactivity, there was no discernible [^{3}H]DAP released from the walls.

FIG. 5. *Cell wall fragment after incubation in F-Con A and spreading on a grid surface. The density is due to the F-Con A, since no other staining reagent has been used.*

FIG. 6. *Same as Fig. 5, but 0.1 M* D*-glucose was added to the reaction mixture. Few F-Con A granules are associated with the wall fragment in comparison to Fig. 5.*

FIG. 7. *Thin section of a wall incubated in 5 mM $MgCl_2 \cdot 6H_2O$ for 10 min at 22°C. Electron scattering is seen in the central region of the wall and measures 16 nm in width (arrows). The remaining two arrows point to unstained peripheral regions of wall, and this has a width of ca. 30 to 35 nm. No stain was used on this section.*

FIG. 8. *Similar to Fig. 7, but F-Con A has been used to label the surfaces of the wall. This confirms that Mg^{2+} stains a central wall component. Arrows give similar dimensions as in Fig. 7.*

FIG. 9. *Similar to Fig. 8, but ruthenium red (500 μg/ml) has been used as an additional stain. Note that the wall contrast has not been increased by this stain. Arrows give similar dimensions as in Fig. 7.*

FIG. 10. *Similar to Fig. 7, but the section has been stained with uranyl acetate-lead citrate. Note that the central region is very dense due to the additive effect of magnesium and the stains. Arrows give similar dimensions as Fig. 7.*

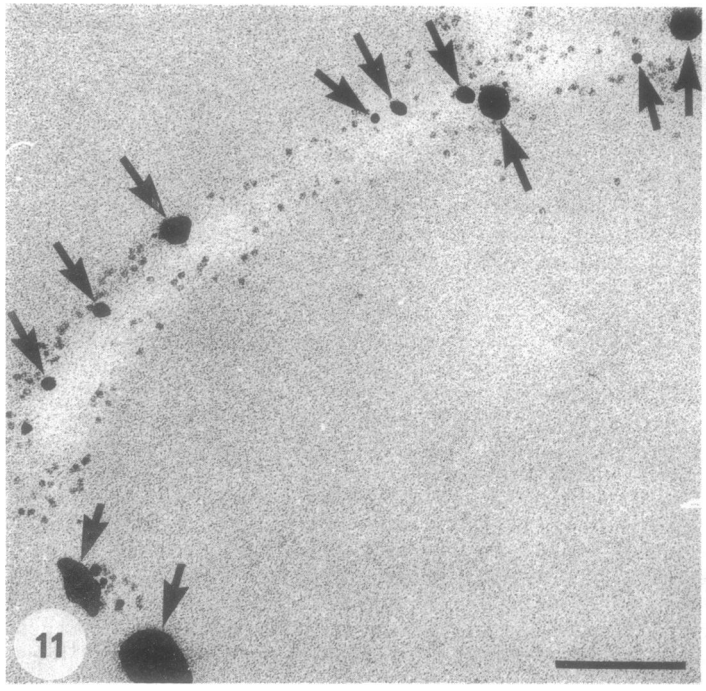

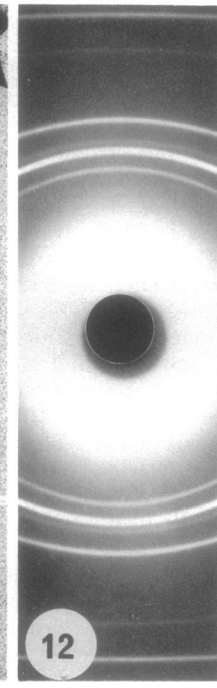

FIG. 11. *Thin section of a wall fragment which was incubated in 5 mM Au $Cl_3 \cdot 2H_2O$ for 5 min at 22°C. The wall surfaces have been labeled with F-Con A and arrows point to the very dense, growing crystals of gold.*

FIG. 12. *X-ray diffraction pattern from wall fragments which were incubated in 5 mM $AuCl_3 \cdot 2H_2O$ for 10 min at 22°C.*

FIG. 13. *Thin section of a wall typical of the preparation which produced the diffraction pattern seen in Fig. 12. No stain other than the auric chloride was used on the wall.*

Metal retention experiments using the affinity chromatographic column technique. The wall fragments cross-linked to AHA beads by carbodiimide (EDC) reaction were firmly bound to the beads and could not be dislodged by sonication of the mixture. In fact, the beads were shattered before the walls were torn from the bead surface. Phase microscopy (Fig. 14A) and thin sections (Fig. 14B) of beads with attached wall fragments (AHA-WF) showed large numbers of fragments on the bead surfaces. Monitoring for radioactivity ([^{3}H]DAP) in the wash fluids and in AHA-WF during several runs indicated that 95 to 98% of the total available was in the AHA-WF fraction, and this activity was not eluted from the column during the course of a metal retention experiment. Higher magnification of thin sections of AHA-WF demonstrated that the EDC reaction had not altered the ultrastructure of the wall fragments and that thin fibrils from the AHA bead extended to the attached surface of the wall (Fig. 15). It was of interest that even a part of the bead substance could be stained by Reynolds' method. Analyses of AHA and AHA-WF for metal uptake indicated that the beads captured no more than 1 to 5% of the total (depending on the metal) and that the cross-linking reaction had reduced the metal-binding capacity of the walls by no more than 1%. This latter observation was more or less confirmed by comparison of the metal retention and uptake values (i.e., compare Mg^{2+}, Ca^{2+}, and Ni^{2+} values in Tables 1 and 3).

Part of Table 3 records the metal retention capacity of the whole cell wall after exposure to a series of metal solutions by assay of the amount of each metal bound to the wall at the completion of the experiment. A surprising amount of metal remained in the walls (i.e., 13.068 μmol of metal per mg (dry weight) of wall fragments) and most of this consisted of firmly bound Mg^{2+} and Fe^{3+}. Other metals which were not easily displaced were Ca^{2+} and Ni^{2+}, whose retention values compared well with the uptake values; and these, together with Mg^{2+} and Fe^{3+}, accounted for 93% of the retained metal in the walls based on micromoles per milligram (dry weight) of wall fragments. This quantity of metal was readily visible in unstained thin sections of the AHA-WF after the metal series had been completed (Fig. 16). In this instance the AHA matrix was not visible (an indication of little or no metal uptake competition between the matrix and cell walls), but the wall fragments exhibited strong electron-scattering ability, the greatest retention of metal occurring at the outer surface of the wall (Fig. 16). Once again ruthenium red (as a staining reagent for thin sections) produced a marginal increase in the density of the fragments which was similar to the Mg^{2+}-incubated walls used in the uptake experiments.

TABLE 2. *Uptake values of B. subtilis wall fragments for Mg^{2+} and Fe^{3+} as determined by atomic absorption analysis after a 42-h incubation at 4°C in various metal concentrations*

Metal	Concn (mM)	Uptake data	
		μg/mg (dry wt) of wall fragments	μmol/mg (dry wt) of wall fragments
Mg^{2+}	0.5	105.8	4.352
	5.0	120.0	4.936
	50.0	140.2	5.767
Fe^{3+}	0.5	4.6	0.082
	5.0	20.0	0.358
	50.0	74.0	1.325

The walls on AHA-WF partially digested by lysozyme lost 28% of their total [^{3}H]DAP and, when thin sectioned, their compact structure had become loosely knit (Fig. 17). Table 3 also shows that these walls retained less than one-third of the metal held by the whole cell walls (i.e., 3.978 μmol/mg [dry weight] of wall fragments compared to 13.068 from the previous experiment). The retention values for all metals, with the exception of Ni^{2+}, were reduced, and in the case of Mg^{2+} the reduction was extreme. Fe^{3+} alone contributed 72% of the retained metal. Thin sections of this material still provided ample electron scattering to visualize the wall fragments, but the loose nature of the wall substance would not allow easy determination of any partitioning of the retained metal (Fig. 18).

DISCUSSION

Cell walls of *B. subtilis* may contain as much as 70% of their dry weight as teichoic acid when grown in phosphate- (14) and glucose-containing medium (F. J. Kruyssen, W. R. de Boer, and J. T. M. Wouters, Proc. Soc. Gen. Microbiol. 3: 30, 1975) and these conditions were used to produce the bacteria for our experiments. This anionic polymer of α-D-glucopyranosyl glycerol phosphate is covalently linked to the peptidoglycan of the wall (25), which itself consists of an alternating polymer of β-(1,4)-linked *N*-acetylglucosamine and *N*-acetylmuramic residues, the latter unit bearing a short peptide side chain [L-Ala-D-Glu-(L)-*meso*-Dpm-D-Ala] of which ca. 35% are cross-linked through D-alanyl-(D)-*meso*-diaminopimelyl bonds to adjacent glycopeptide strands (49).

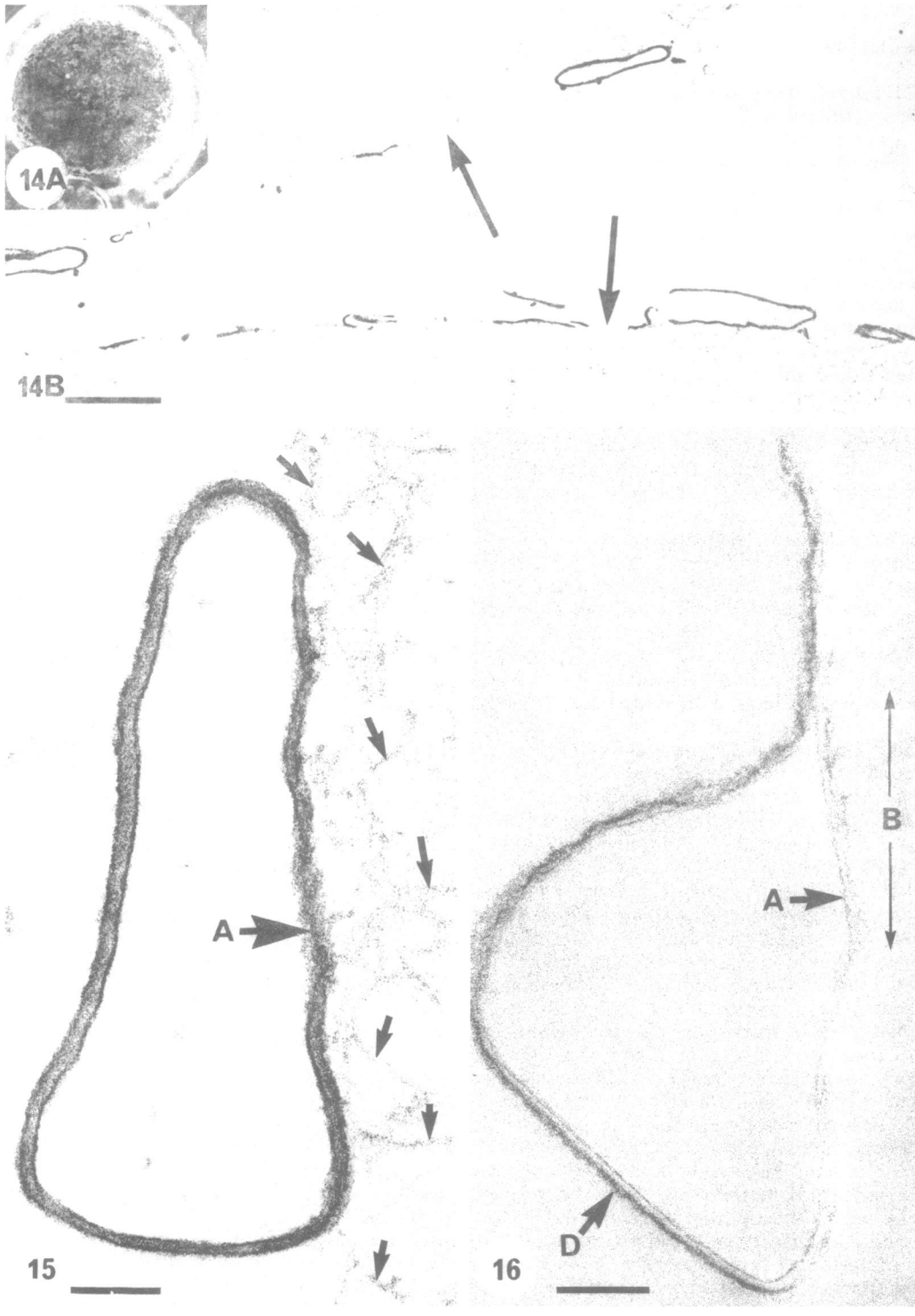

FIG. 14. *(A) Phase micrograph of an adipic-hydrazide-agarose bead with attached wall fragments (AHA-WF) after carbodiimide reaction. ×700. (B) Thin section of portions of an AHA-WF bead. The arrows are pointing to the bead surface on which many wall fragments are attached. This and Fig. 15 and 17 are stained with uranyl acetate-lead citrate. The marker bar = 1 μm.*

FIG. 15. *High-magnification profile of an attached wall fragment stained with uranyl acetate-lead citrate. Arrows point to the fibrils of the AHA. A, Attached surface of the wall fragment.*

FIG. 16. *Same as Fig. 15, but without additional staining after the 10 metals of the metal retention experiment have been passed through the AHA-WF matrix. B, Unstained AHA surface; A, attached surface of wall fragment; D, surface density of wall.*

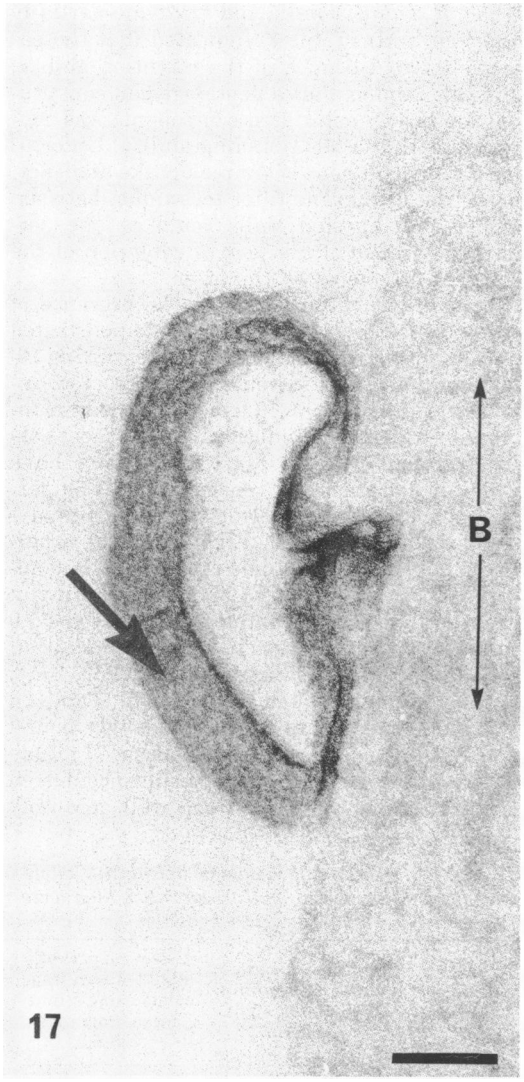

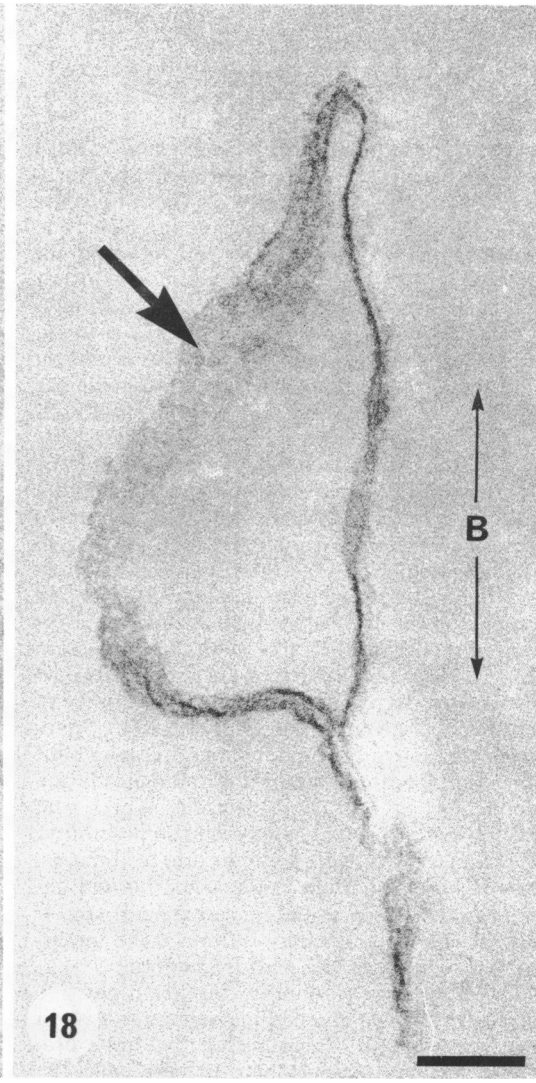

FIG. 17. *A wall fragment of AHA-WF after partial lysozyme digestion. B, AHA surface; large arrow points to the loose-knit cell wall.*

FIG. 18. *Same as Fig. 17, but unstained and after exposure to the 10 metals of a metal retention experiment. B, Unstained AHA surface; arrow points to fabric of wall.*

The wall fragments exposed to metal solutions behaved, for the most part, as nonspecific ionophores, since a variety of metals was absorbed by the wall substance (Table 1). This behavior was not in itself surprising, since many potential anionic sites are available in and on the wall, i.e., the teichoic phosphodiester groups (24), the free carboxyl groups of the peptidoglycan (in particular, the carboxyls of the glutamic residues and also of the DAP of one strand and the C-terminal D-alanine of the other [47]), and, to a lesser extent, the sugar hydroxyl groups of both wall polymers and the amide groups of peptide chains (46). However, the extreme uptake of several metals was unexpected and could readily be verified by their electron-scattering properties in thin-sectioned material.

Magnesium is an element of low atomic number and cannot be expected to scatter electrons to any degree unless unusually large quantities are present, and these amounts were found in the central region of the wall (Fig. 7). Subsequent preparations indicated that this image was not an artifact (Fig. 8 and 10). This sequestering of the metal into a specific region of the

wall implied a degree of macromolecular arrangement hitherto undetected in *B. subtilis* (this region differing in at least its ability to trap Mg^{2+}). The difficulty of enhancing the contrast of the image with ruthenium red (Fig. 9) may imply that some Mg^{2+} was bound to wall teichoic acid (19), thereby reducing the numbers of available binding sites in the wall to the stain. Ruthenium red stain alone increased the scattering power of the entire cell wall and not just the central region, which could argue that the teichoics extend through the wall substance. Studies using *Staphylococcus aureus, Micrococcus* sp. 24, and *Lactobacillus buchneri* have indicated that teichoic phosphodiester groups can bind quantities of Mg^{2+} (24, 33) but not of the same order as our results. These facts lead us to suspect that teichoic acid is not the only chelating agent for Mg^{2+} in *B. subtilis* walls. Recently Rayman and MacLeod have provided data on the interaction of Mg^{2+} with the peptidoglycan of a marine pseudomonad and have suggested that a bidentate chelate complex is formed between two peptide chains from adjacent murein strands and magnesium (47). Other studies, using walls of *Bacillus psychrophilus,* have suggested the availability of the carboxyl group of the lactyl moiety of nonpeptidized muramic acid for metal entrapment (4). After chemical analysis of the degradation products of *B. subtilis* cell walls, Warth and Strominger (49) have suggested the possibility of a third type of wall polymer due to the presence of large amounts of glucosamine and galactosamine (in excess of muramic acid), and if present this polymer may influence the metal-trapping ability of the wall fragments.

The possibility of whether the gram-positive cell wall exists as an open ion-exchange system is of open debate. Some authorities have presented data in support of this view (43, 44), whereas, more recently, Formanek et al. have suggested that it is a condensed system (17). The large uptake values and specificity of retention seen in our results with the *B. subtilis* cell wall indicate that this system is more closely allied with a condensed form with a specificity of sites for discrete cationic species. It is encouraging to note that the recent models for bacterial mucopeptide have a condensed format (17). With respect to the *B. subtilis* cell wall it is our feeling that to label it either "open" or "condensed" may be too simplistic, since several subtle factors dealing with water chemistry and/or water structure, metal complexing, interfacial phenomena, etc. may also be involved in the total metal uptake.

Comparison of magnesium retention between whole *B. subtilis* walls and lysozyme-partially digested walls (Table 3) indicated that the enzyme destroyed much of the retention ability, and this implies that a peptidoglycan constituent (or closely associated component) was connected with the Mg^{2+}-binding ability. Unfortunately, comparisons of simple uptake analyses, using the membrane filter technique, between whole and digested walls could not be performed because of the lack of retention of the digested fragments by the filter.

Longer incubation times in the presence of three concentrations of Mg^{2+} demonstrated only slightly increased Mg^{2+} uptakes during 10-fold concentration increases (i.e., ca. 15% increased uptake for a 10-fold concentration increase), which may indicate that the most easily available sites for Mg^{2+} entrapment have been filled at the lower concentration. Comparison of the combined atomic absorption analyses of the retentate plus filtrate after the experiment suggested that some magnesium had adsorbed to the plastic of the syringe, resulting in the overall decreased uptakes (compare the 5.0 mM Mg^{2+} uptake values in Tables 1 and 2).

Substantial quantities of Fe^{3+}, Cu^{2+}, Na^{+}, and K^{+} were also taken into the wall (Table 1), but Fe^{3+} appeared to be more strongly bound since the other metals could be replaced (Table 3). Iron uptake, unlike magnesium, conferred diffuse density throughout the wall, and only

TABLE 3. *Retention of metals of B. subtilis whole and lysozyme-digested wall fragments which were bound to AHA beads*

Order of application of 5 mM metal solutions	Metals	Whole wall fragments using affinity chromatographic column		Lysozyme-partially digested wall fragments using affinity chromatographic column	
		μg of metal/mg (dry wt) of wall fragments	μmol of metal/mg (dry wt) of wall fragments	μg of metal/mg (dry wt) of wall fragments	μmol of metal/mg (dry wt) of wall fragments
	Li^{+}	0	0	0	0
	Na^{+}	0.97	0.042	0.19	0.008
	K^{+}	2.30	0.590	0.66	0.017
	Mg^{2+}	200.00	8.226	10.00	0.411
	Ca^{2+}	16.00	0.399	13.60	0.339
	Sr^{2+}	2.15	0.025	1.60	0.018
	Ba^{2+}	0	0	0	0
	Fe^{3+}	189.00	3.384	160.00	2.865
	Cu^{2+}	18.80	0.296	13.30	0.209
	Co^{2+}	0	0	0	0
	Mn^{2+}	0	0	0	0
	Ni^{2+}	6.2	0.106	6.5	0.111

rarely were highly scattering wall crystaloids seen after short incubation periods (Fig. 4B); however, this was not the case for longer incubations where copious crystaloids were revealed in thin sections. Atomic absorption analyses of the walls after these longer incubations demonstrated that greatly reduced quantities of iron were retained by the filter (Table 2), and this implied that some of the bound iron (which was seen after a 10-min incubation) had been leached from the walls. Fe^{3+} is an unstable aquo-ion in solution (except in strongly acidic conditions) and may undergo a series of hydrate transition states, one of which is the insoluble oxide hydrate (3). It is possible that the walls were demonstrating a two-step process during the 42-h incubation; the first event in time may involve the capturing of discrete and unstable iron hydroxide species by the anionic wall fragments, and the second may involve the formation of crystaloids (presumably an aggregate of iron oxide hydrate initiated by event no. 1) on the surface of the wall. Once these crystaloids had formed, they should have provided a more thermodynamically favored site which, by equilibration and time, would leach the dispersed iron species from the interior of the wall. If this was the case, any wall-bound iron leaving its secure position would be captured by the growing crystaloids until very little was left in the walls, and this was substantiated by the lowered uptake values and a decrease in the electron-scattering power of the 42-h walls. During the filtration process preliminary to atomic absorption analysis most of the crystaloids ($<< 0.22$ μm) would be found in the filtrate, thereby producing the low iron yields of the walls. On the other hand, during a metal retention experiment (i.e., affinity chromatographic column experiment) the continual movement of solution and wash through the AHA-WF would not allow aggregates of iron oxide hydrate to become established and accumulate, and therefore the competition process would not be able to potentiate leaching of iron (Table 3).

The uptake of gold appeared to be a unique process which was not shared by the other metals. Au^{3+} is also unstable in aqueous environments, and its halides are readily hydrolyzed in water to form hydrous auric oxide precipitates (50). X-ray diffraction analysis of Au^{3+}-incubated wall fragments demonstrated that they contained elemental gold and not the oxide (Fig. 12) and suggested that this was not a simple precipitation process. In fact, thin sections of these walls revealed that initiation of the uptake began at discrete points in the wall substance and grew, as crystals, until they extended beyond the limits of the wall fragment (compare Fig. 11 and 13), which indicated a two-step process (i.e., [i] discrete regions in the wall substance captured enough Au^{3+} to initiate [ii], a seeding process for the crystallization of elemental gold). If this process was in fact at work, then the eventual bound gold concentration would not be an accurate indication of available sites for Au^{3+}, but a combination of the gold contributed by both processes.

After they had been suspended in the various metal solutions, thin sections of the walls, without exception, could be further stained by the uranyl acetate-lead citrate method (48). This fact suggested that either some sites were still available in the wall or that the UO_2^{2+} or Pb^{2+} ions could replace the other metals. Although we have no uptake values for the uranyl ion, Pb^{2+} was poorly taken into the wall substance (i.e., 0.020 μmol/mg [dry weight] of wall fragments), but this was at much lower pH than Reynolds' reaction [i.e., pH of $Pb(NO_3)_2$ wall fragment suspension was 4.5 compared to pH 12.0 for the Pb citrate stain]. The sequence of the staining solutions for the thin sections was 2% uranyl acetate at low pH (e.g., pH 4.0, and this cannot be higher unless a chelating agent is added [23]) and then the high-pH Pb citrate stain. These two extremes in pH may have affected the number of sites in the wall normally available and/or displaced the metal with either the UO_2^{2+} or Pb^{2+} of the staining solutions. This mechanism, of course, did not dislodge all of the Mg^{2+} from the central wall region which was strongly bound (Fig. 10).

Most charge-free spacer gels have been used for the immobilization of relatively small ligands such as nucleotides (34) and proteins (29), and to our knowledge this is the first application of this technique to complex structural entities such as whole bacterial wall fragments. Experiments in our laboratory indicate that it may also be applied to whole cells (T. Beveridge and T. Jack, unpublished observations). Using a variety of gels, we have observed that the AHA beads provide copious numbers of linked wall fragments on the bead surface, suitable "flow rate" in the column, and minimal uptake of the metals. When linked to AHA the walls lost no more than 1% of their ability to bind metals, and this loss was presumably due to the covalent bonds established between surface wall carboxyl groups and the hydrazide groups of the AHA during the carbodiimide reaction. The presence of excess water during the reaction means that this water acts as a nucleophile to regenerate most unlinked

carboxyl groups in the wall during the conversion of the carbodiimide to its urea end product (9), thereby maintaining carboxyl availability for metal interaction.

When a series of 12 metal solutions was passed through AHA-WF columns it became evident that Mg^{2+}, Ca^{2+}, Fe^{3+}, and Ni^{2+} were strongly bound to the wall fragments, which suggests that their binding sites must differ. Conversely, Na^{+}, K^{+}, Cu^{2+}, and Mn^{2+} must have been lost in competition with another metal ion for their binding site. Partial lysozyme digestion of AHA-WF reduced the retention values of all but Ni^{2+} and, for Mg^{2+}, this reduction was drastic (Table 3). This was evidence that the peptidoglycan (or some closely associated constituent) contributed to the metal-binding ability of the wall substance. We hope to further elucidate the sites of metal-wall interaction.

If one thinks in terms of a condensed verus an open ion-exchange system for the *B. subtilis* cell wall, it may very well be that the lysozyme digestion has in fact converted a relatively condensed system to a more open one, and this could explain, in part, the drastic reduction and specificity of total bound metal in the digested walls. It is of interest to note that thin sections of these walls suggest a more loosely knit structure (Fig. 17 and 18).

The gram-positive cell wall has been compared to a low-density, ion-exchange resin (43, 44), and its hydrophobic areas have been compared to traps for the binding of hydrophilic molecules (10). Metal cations could profoundly influence the hydrophobic-hydrophilic nature of the wall as well as its electrical characteristics, and the degree and type of metal binding to the wall would be a function of the external accessibility of metal ion species and the strength of binding. The limiting porosity of *Bacillus megaterium* plasma membrane is ca. 0.6 nm, but this is reduced by the addition of Mg^{2+} (20), and if these walls are similar to *B. subtilis*, then the wall magnesium content may profoundly affect the permeability of the membrane. In the case of *B. subtilis*, Ca^{2+}, Mg^{2+}, and La^{2+} have the ability to confer rigidity on the membrane (13). Graphical analyses of changes in the molecular weight distribution of a single polydisperse polymer sample before and after its uptake in *B. megaterium* cells have demonstrated that the wall porosity is bilayered (i.e., the Einstein-Stokes hydrodynamic radii of outer, middle, and inner regions of the wall were 1.1, 3.0, and 27.0 nm, respectively [20]), and it is possible that this change in porosity may affect, or be affected by, metal ions in the wall. It is striking that a bilayered partitioning occurred with the magnesium in the wall fragments of *B. subtilis* (Fig. 7).

No simple electrostatic explanation of the binding of a metal ion to a ligand is satisfactory, since the preference for a particular ligand is a function of the cation in aqueous solution, and this can become highly selective if not specific (52). For this reason each metal may bind to a unique set of sites in the wall, possibly by different mechanisms, and therefore simple comparisons of uptake values may not have a common basis. Some of the characteristics which influence the selection of one ligand over another are size of cation, electronegativity, and gross steric factors of the ligand (52), and, of great importance in aqueous chemistry, the heat of hydration and size and/or arrangement of the hydration shell (3, 51). Those metals absorbed by the wall fragments can be arranged in order of the quantities of uptake (in micromoles per milligram [dry weight] of wall fragments) and compared in terms of their ionic radii, heats of hydration, and number of water molecules in their hydration shells (Table 4). No simple correlation of these three variables with uptake values could be made. A direct comparison of Fe^{3+} or Au^{3+} with the other cations was impossible, since in the former its interaction with water is unique and complex and in the latter elemental crystalization occurred. Crystal field stabilization energy introduces a subtle complexity which makes direct comparisons between transition metal ions and the alkali or alkali earth metal ions difficult, and this in part may account for the lack of simple correlation between the remaining metals. Ignoring such contributions, we may make a few observations; with the exception of Co^{2+}, the metals which were not taken up by the walls possessed either extremely large or small ionic radii (e.g., Ba^{2+} or Al^{3+}) or heats of hydration (e.g., Li^{+} or Al^{3+}) when compared to those metals which were taken up. In the case of the monovalent cations the uptakes were $Li^{+} << Na^{+} \sim K^{+} > Ag^{+}$, and it is interesting to note that Li^{+} possesses the smallest ionic radius and the largest heat of hydration of this group. If the 2+ or 3+ metals are considered, we find that, with the exception of Co^{2+} whose aqueous chemistry is unclear, extreme size (large or small) and/or extreme heats of hydration may be factors. Since no attempt was made to control pH or redox potential in these experiments the aqueous metal species (especially with the transition metals) involved in the reaction is at present unclear, and this too makes simplistic interpretations difficult.

This communication has shown that some

TABLE 4. *Order of the uptake of the various metals, their ionic radii, and heats of hydration*[a]

Characteristic	Large uptake → Small uptake → No uptake																
	Mg^{2+}	Fe^{3+}	Cu^{2+}	Na^{+}	K^{+}	Mn^{2+}	Zn^{2+}	Ca^{2+}	Au^{3+}	Ni^{2+}	Hg^{2+}	Ag^{+}	Sr^{2+}	Pb^{2+}	Li^{+}	Ba^{2+}	Co^{2+}	Al^{3+}
Ionic radius (A)	0.78	0.67	0.72	0.95	1.33	0.91	0.83	0.99		0.78	1.12	1.13	1.27	0.80	0.78	1.43	0.82	0.57
−Heat of hydration /kcal at 25°C)	464	1072	507	100	79	445	492	382		507	441	116	350	505	125	316	497	1122
No. of H_2O in hydration shell	6	6	4	4	4 or 6	6	6	6		6					4		6	6

Complex water chemistry

Crystal formation as elemental gold

[a] References 3 and 50.

diverse metals are selectively trapped (in some cases very tenaciously) in the cell wall of a ubiquitous gram-positive bacterium. Traces of microbes and considerable concentrations of metals have been found in sediments from ancient geological horizons (e.g., the isoprenoid hydrocarbons from the precambrian Nonesuch formation [12], the mineralized remains of microorganisms from the Precambrian Gunflint chert of northern Lake Superior [2], and possible microfossils from Precambrian iron formations found in the United States, Canada, Australia, and South Africa [32]), and these are usually closely associated with metal deposits, often of large proportions. The exact manner of deposition of these metals is of open debate, and the associated microbial remnants lead one to speculate as to the possibility of their biological origin.

This phenomenon is now described, but the physicochemical basis for selectivity and tenacity is obscure. Experiments are in progress controlling pH and redox potential, modifying or blocking various reactive groups in the wall, and assessing the influence of various wall components.

ACKNOWLEDGMENTS

We are indebted to The Richard Ivey Foundation for funding this research; to the Medical Research Council of Canada for support of the electron microscope unit; to W. S. Fyfe, J. E. Zajic, T. R. Jack, and B. J. Fryer for their interest and help during the research; and to C. Schaap, M. Luney, and H. Koppenhoeffer for technical assistance.

LITERATURE CITED

1. **Agrawal, B. B. L., and I. J. Goldstein.** 1967. Protein-carbohydrate interaction. VI. Isolation of concanavalin A by specific adsorption on cross-linked dextran gels. Biochim. Biophys. Acta 147:262-271.
2. **Banghoorn, E. S., and S. A. Tyler.** 1965. Microorganisms from the gunflint chert. Science 147:563-577.
3. **Basolo, F., and R. G. Pearson.** 1972. Mechanics of inorganic reactions, 2nd ed., p. 81-82, 198. John Wiley & Sons, Inc.-Interscience Publishers, Inc., New York.
4. **Best, G. K., and S. J. Mattingly.** 1973. Chemical analysis of cell walls and autolytic digests of *Bacillus psychrophilus*. J. Bacteriol. 115:221-227.
5. **Beveridge, T. J., and R. G. E. Murray.** 1976. Reassembly *in vitro* of the superficial cell wall components of *Spirillum putridiconchylium*. J. Ultrastruct. Res. 55:105-118.
6. **Beveridge, T. J., and R. G. E. Murray.** 1976. Superficial cell wall layers on *Spirillum* "Ordal" and their *in vitro* reassembly. Can. J. Microbiol. 22:567-582.
7. **Birdsell, D. C., R. J. Doyle, and M. Morgenstern.** 1975. Organization of teichoic acid in the cell wall of *Bacillus subtilis*. J. Bacteriol. 121:726-734.
8. **Buckmire, F. L. A., and R. G. E. Murray.** 1976. The substructure and in vitro assembly of the outer, structured layer of *Spirillum serpens*. J. Bacteriol. 125:290-299.
9. **Carraway, K. L., and D. E. Koshland, Jr.** 1972. Carbodiimide modification of proteins, p. 616-623. *In* C. H. W. Hirs and S. N. Timasheff (ed.), Methods in enzymology, vol. 25B. Academic Press Inc., New York.
10. **Doyle, R. J., A. N. Chatterjee, U. N. Streips, and F. E. Young.** 1975. Soluble macromolecular complexes involving teichoic acids. J. Bacteriol. 124:341-347.
11. **Doyle, R. J., M. L. McDannel, J. R. Helman, and U. N. Streips.** 1975. Distribution of teichoic acid in the cell wall of *Bacillus subtilis*. J. Bacteriol. 122:152-158.
12. **Eglinton, G., P. M. Scott, T. Belsky, A. L. Burlingame, and M. Calvin.** 1964. Hydrocarbons of biological origin from a one-billion-year-old sediment. Science 145:263-264.
13. **Ehrström, M., L. E. Göran Eriksson, J. Israelachvii, and A. Ehrenberg.** 1973. The effects of some cations and anions on spin labeled cytoplasmic membranes of *Bacillus subtilis*. Biochem. Biophys. Res. Commun. 55:396-402.
14. **Ellwood, D. C., and D. W. Tempest.** 1969. Control of teichoic acid and teichuronic acid biosynthesis in chemostat cultures of *Bacillus subtilis* var. niger. Biochem. J. 111:1-5.
15. **Fiil, A., and D. Branton.** 1969. Changes in the plasma membrane of *Escherichia coli* during magnesium starvation. J. Bacteriol. 98:1320-1327.
16. **Fontana, R., G. Satta, L. Caligari, and C. A. Romanzi.** 1974. The murein-lipoprotein of *Klebsiella pneumoniae* MIR AI2 and its morphology mutant MIR M7. Proc. Intersect. Cong. I.A.M.S. 1:486-490.

17. **Formanek, H., S. Formanek, and H. Wawra.** 1974. A three-dimensional atomic model of the murein layer of bacteria. Eur. J. Biochem. 46:279–294.
18. **Fortnagel, P., and E. Freese.** 1968. Analysis of sporulation mutants. II. Mutants blocked in the citric acid cycle. J. Bacteriol. 95:1431–1438.
19. **Garland, J. M., A. R. Archibald, and J. Baddiley.** 1975. An electron microscopic study of the location of teichoic acid and its contribution to staining reactions in the walls of *Streptococcus faecalis* 8191. J. Gen. Microbiol. 89:73–86.
20. **Gerhardt, P., and R. Scherrer.** 1974. Porosities of microbial cell walls and protoplast membranes. Proc. Intersect. Cong. I.A.M.S. 1:506–513.
21. **Gerrard, T. L., J. N. Telford, and H. H. Williams.** 1974. Detection of selenium deposits in *Escherichia coli* by electron microscopy. J. Bacteriol. 119:1057–1060.
22. **Gilleland, H. E., Jr., J. D. Stinnett, and R. G. Eagon.** 1974. Ultrastructural and chemical alteration of the cell envelope of *Pseudomonas aeruginosa*, associated with resistance to ethylenediaminetetraacetate resulting from growth in a Mg^{2+}-deficient medium. J. Bacteriol. 117:302–311.
23. **Hayat, M. A.** 1975. Positive staining for electron microscopy, p. 17–44. Van Nostrand Reinhold Co., New York.
24. **Heptinstall, S., A. R. Archibald, and J. Baddiley.** 1970. Teichoic acids and membrane function in bacteria. Selective destruction of teichoic acid reduces the ability of bacterial cell walls to bind Mg^{2+} ions. Nature (London) 225:519–521.
25. **Hughes, R. C.** 1970. Autolysis of isolated cells walls of *Bacillus licheniformis* N.C.T.C. 6346 and *Bacillus subtilis* Marburg strain 168. Separation of the products and characterization of the mucopeptide fragments. Biochem. J. 119:849–860.
26. **Humphrey, B. A., and J. M. Vincent.** 1966. Strontium as a substituted structural element in cell walls of *Rhizobium*. Nature (London) 212:212–213.
27. **Irvin, R. T., A. K. Chatterjee, K. E. Sanderson, and J. W. Costerton.** 1975. Comparison of the cell envelope structure of a lipopolysaccharide-defective (heptose-deficient) strain and a smooth strain of *Salmonella typhimurium*. J. Bacteriol. 124:930–941.
28. **Jernelöv, A., and A-L. Martin.** 1975. Ecological implications of metal metabolism by microorganisms. Annu. Rev. Microbiol. 29:61–77.
29. **Jost, R., T. Miron, and M. Wilchek.** 1974. The mode of adsorption of proteins to aliphatic and aromatic amines coupled to cyanogen bromide-activated agarose. Biochim. Biophys. Acta 362:75–82.
30. **Ketchum, P. A., and M. S. Owens.** 1975. Production of a molybdenum-coordinating compound by *Bacillus thuringiensis*. J. Bacteriol. 122:412–417.
31. **Konings, W. N., and E. Freese.** 1971. L-serine transport in membrane vesicles of *Bacillus subtilis* energized by NADH or reduced phenazine methosulfate. FEBS Lett. 14:65–68.
32. **La Berge, G. L.** 1967. Microfossils and precambrian iron-formations. Geol. Soc. Am. Bull. 78:331–342.
33. **Lambert, P. A., I. C. Hancock, and J. Baddiley.** 1975. The interaction of magnesium ions with teichoic acid. Biochem. J. 149:519–524.
34. **Lamed, R., Y. Levin, and M. Wilchek.** 1973. Covalent coupling of nucleotides to agarose for affinity chromatography. Biochim. Biophys. Acta 304:231–235.
35. **Luft, J. H.** 1971. Ruthenium red and violet. I. Chemistry, purification and methods for usesin electron microscopy and mechanism of action. Anat. Rec. 171:347–368.
36. **Macham, L. P., and C. Ratledge.** 1975. A new group of water-soluble iron-binding compounds from mycobacteria: the exochelins. J. Gen. Microbiol. 89: 379–382.
37. **Mulder, E. G.** 1974. Genus *Leptothrix* Kützing 1843, 198, p. 129–133. *In* R. E. Buchanan and N. E. Gibbons (ed.), Bergey's manual of determinative bacteriology, 8th ed. The Williams & Wilkins, Co., Baltimore.
38. **Mulder, E. G., and M. L. van Veen.** 1974. Genus *Sphaerolilus* Kützing 1833, 386, p. 128–129. *In* R. E. Buchanan and N. E. Gibbons (ed.), Bergey's manual of determinative bacteriology, 8th ed. The Williams & Wilkins Co., Baltimore.
39. **Nicolson, G. L., and S. J. Singer.** 1971. Ferritin-conjugated plant agglutinins as specific saccharide stains for electron microscopy: application to saccharides bound to cell membranes. Proc. Natl. Acad. Sci. U.S.A. 68:942–945.
40. **Osada, Y., T. Une, T. Ikeuchi, and H. Ogawa.** 1974. Effect of calcium on the cell infectivity of virulent *Shigella flexneri* 2a. Jpn. J. Microbiol. 18:321–326.
41. **Osada, Y., T. Une, T. Ikeuchi, and H. Ogawa.** 1975. Divalent cation stimulation of cell infectivity of *Shigella flexneri* 2a. Jpn. J. Microbiol. 19:163–166.
42. **Osborn, M. J., K. E. Gander, and E. Parisi.** 1972. Mechanism of assembly of outer membrane of *Salmonella typhimurium*: isolation and characterization of cytoplasmic and outer membrane. J. Biol. Chem. 247:3973–3986.
43. **Ou, L-T., and R. E. Marquis.** 1970. Electromechanical interactions in cell walls of gram-positive cocci. J. Bacteriol. 101:92–101.
44. **Ou, L-T., and R. E. Marquis.** 1972. Coccal cell wall compactness and the swelling action of denaturants. Can. J. Microbiol. 18:623–629.
45. **Postgate, J. R.** 1968. Fringe biochemistry among microbes. Proc. R. Soc. London Ser. B 171:67–76.
46. **Rao, C. N. R., K. G. Rao, and D. Balasubramanian.** 1974. Binding of alkali and alkaline earth cations and of the protons to the peptide group. FEBS Lett. 46:192–194.
47. **Rayman, M. K., and R. A. MacLeod.** 1975. Interaction of Mg^{2+} with peptidoglycan and its relation to the prevention of lysis of a marine pseudomonad. J. Bacteriol. 122:650–659.
48. **Reynolds, E. S.** 1963. The use of lead citrate at high pH as an electron-opaque stain in electron microscopy. J. Cell Biol. 17:208–212.
49. **Warth, A. D., and J. L. Strominger.** 1971. Structure of the peptidoglycan from vegetative cell walls of *Bacillus subtilis*. Biochemistry 10:4349–4358.
50. **Weast, R. C.** 1969. CRC handbook of chemistry and physics, 49th ed., p. B97–B265. Chemical Rubber Co., Cleveland.
51. **Williams, D. R.** 1971. Metals of life. Van Nostrand Reinhold Co., New York.
52. **Williams, R. J. P.** 1961. Nature and properties of metal ions of biological interest and their coordination compounds. Fed. Proc. 20(Suppl. 2):5–14.